Internal solitary waves of elevation advancing on a shoaling shelf

Jody M. Klymak and James N. Moum

College of Oceanic and Atmospheric Sciences, Oregon State University, Corvallis, Oregon, USA

Received 8 May 2003; accepted 17 September 2003; published 23 October 2003.

[1] A sequence of three internal solitary waves of elevation were observed propagating shoreward along a near-bottom density interface over Oregon's continental shelf. These waves are highly turbulent and coincide with enhanced optical backscatter, consistent with increased suspended sediments in the bottom boundary layer. Non-linear solitary wave solutions are employed to estimate wave speeds and energy. The waves are rank ordered in amplitude, phase speed, and energy, and inversely ordered in width. Wave kinetic energy is roughly twice the potential energy. The observed turbulence is not sufficiently large to dissipate the waves' energy before the waves reach the shore. Because of high wave velocities at the sea bed, bottom stress is inferred to be an important source of wave energy loss, unlike near-surface solitary waves. The wave solution suggests that the lead wave has a trapped core, implying enhanced cross-shelf transport of fluid and biology. *INDEX TERMS:* 4544 Oceanography: Physical: Internal and inertial waves; 4219 Oceanography: General: Continental shelf processes; 4568 Oceanography: Physical: Turbulence, diffusion, and mixing processes; 4524 Oceanography: Physical: Fine structure and microstructure; 4558 Oceanography: Physical: Sediment transport. **Citation:** Klymak, J. M., and J. N. Moum, Internal solitary waves of elevation advancing on a shoaling shelf, *Geophys. Res. Lett.*, *30*(20), 2045, doi:10.1029/2003GL017706, 2003.

1. Introduction

[2] Non-linear propagating internal solitary waves (ISWs) are a ubiquitous feature of the coastal ocean. They have been observed as sharp depressions of a near surface pycnocline that are often seen at the surface as alternating bands of slicks and rough patches [i.e., *Apel et al.*, 1985; *Moum et al.*, 2003]. When there is a pycnocline near the sea floor, we expect that strong disturbances will manifest themselves as waves of elevation; however, this has rarely been observed [*Bogucki et al.*, 1997; *Wiebe et al.*, 2000].

[3] Here we present an example of solitary waves of elevation propagating shoreward on a continental shelf. We measure both density and turbulence with our profiler chameleon, yielding the first microstructure estimates through ISWs of elevation. These profiles, coupled with coincident acoustic backscatter imaging, provide a unique picture of the structure and energetics of these waves.

2. Experiment

[4] The data presented here were collected in January 2003 over the Oregon shelf. During the experiment, the *R/V Revelle* repeatedly transited a 35 km line along 45°N between the 250 m and 30 m isobaths in order to characterize the winter shelf circulation (Figure 1). Narrow-band acoustic Doppler profiler (ADP, 150 kHz RD Instruments) data is initially smoothed 150 s temporally and 8 m vertically. Single beam echosounder data (120 kHz Biosonics) is smoothed to 14 s in time and 22 cm vertically. Turbulence, conductivity, temperature, optical backscatter, and pressure were sampled with our free-falling profiler chameleon [*Moum et al.*, 1995]. Chameleon is able to profile into the bottom, making it ideal for measuring near-bottom processes.

[5] Here we discuss a transect made between 1645 28 January and 0049 29 January 2003 (UT). The winds had been downwelling favorable (southerly), pushing the bottom boundary layer offshore, but a day previous had switched to upwelling favorable (northerly). Along-shelf currents were approximately barotropic and southward at 0.1 m s^{-1} in the region of interest; cross-shelf currents were small relative to the ISW currents. The water column was weakly stratified; density changed less than 0.6 kg m^{-3} in the upper 70 m. A strong density gradient below σ_θ = 25 kg m^{-3} separated shelf water from deeper water (σ_θ + 1000 kg m^{-3} is the potential density). The dense water formed a front offshore of −8 km, and a tongue of dense water intruded onshore until σ_θ = 25 kg m^{-3} intersected the bottom at +3 km. This stratification is apparently typical of the Oregon shelf during winter [i.e., *Huyer et al.*, 1979, Figure 15].

3. Observations

[6] A train of ISWs were observed at the head of the density front at 120 m depth (x = 0 km, Figure 1). These waves appear as unresolved spikes in density contours derived from the profiler. Their structure is more fully seen in the echosounder (Figure 2), illuminated by a scattering layer found in the density interface starting at ≈114 m depth at −1.3 km. The waves elevate the scattering layer by 15 to 30 m, rank-ordered with the largest amplitude ISW at the front. Their horizontal scales are in opposite order; the tallest wave is the thinnest.

[7] Chameleon profiles indicate the coincidence of the sharp density interface with the scattering layer (white profiles, Figure 2). Above the interface σ_θ = 24.7 kg m^{-3} and stratification is weak ($N^2 \approx 10^{-6}$ s^{-2}). Below the interface σ_θ = 25.55 kg m^{-3} and more stratified. The interface itself is 10 m to 13 m thick ($N^2 \approx 8 \times 10^{-4}$ s^{-2}); its top corresponds well with the scattering layer in the acoustics image.

[8] Velocity data demonstrates that the waves move onshore. Shipboard ADP cannot measure the bottom 20 m of the water column due to sidelobe interference. Wave

0094-8276/03/2003GL017706$05.00

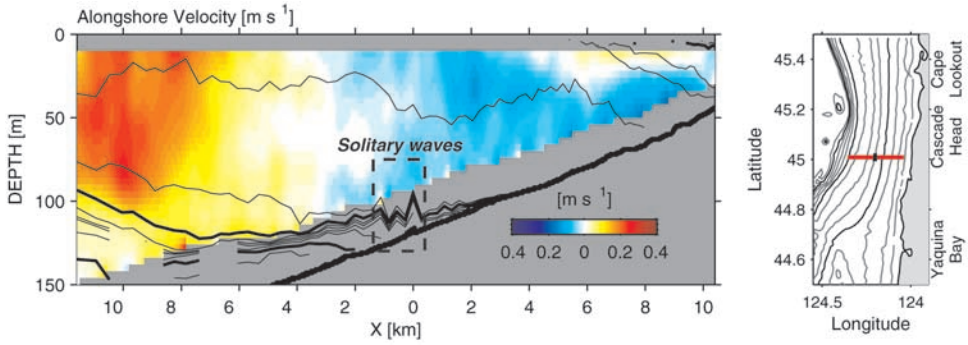

Figure 1. Section of potential density and north-south velocity across the Oregon shelf at 45°N. Beginning at the west end on 1645 28 January 2003 and ending at 0049 29 January (UT). Contour lines of isopycnals are drawn in intervals of 0.2 kg m^{-3}; 26 and 25 kg m^{-3} are drawn thicker. The colored image represents ADP velocities (further smoothed to 6 minutes in time and 12 m in depth). The area of interest is within the dashed box near 0 km (124.20°W). A local map is shown at right with the occupied transect as a red line off Cascade Head.

direction is inferred from velocity data above the waves. The upper tip of the first wave has a pulse of ≈0.2 m s^{-1} onshore velocity that is visible in the ADP (Figure 3a). Above the peak onshore velocity is a weak compensating return flow. The next two waves are not as tall, and the onshore flow cannot be seen. However, offshore return-flows are clear above both these waves. All three waves induce an alternating vertical velocity in the water column (Figure 3b); upward on the leading edge of the wave and downward on the trailing edge.

[9] Beneath the sharp, near-bottom density interface which defines the ISWs the bottom boundary layer exhibits elevated levels of turbulence (black traces, Figure 2). The turbulent kinetic energy dissipation rate $\epsilon \approx 10^{-6}$ m^2 s^{-3} in the front two waves, two orders of magnitude greater than the background $\epsilon < 10^{-8}$ m^2 s^{-3}. Energetic turbulence extends from the density interface to the sea floor. The last wave is less turbulent, characterized by $\epsilon \approx 10^{-7}$ m^2 s^{-3}.

[10] Acoustic backscatter in Figure 2 is likely of biological origin and not turbulence. Microstructure backscatter cross-section estimates [*Seim et al.*, 1995] are below the noise level of the echo-sounder [*Moum et al.*, 2003]. Therefore we expect that the waves are outlined in acoustic images by biological scatterers that have accumulated on the pycnocline. The large cloud of scatterers inside the first wave and at −0.35 km are dense accumulations of zooplankton or small fish.

[11] Optical backscatter is much higher near the bottom within the waves and offshore along the shelf-break front to $x = -30$ km (Figure 4). Optical backscatter at 880 nm is typically associated with small particles like suspended silt or clay. This suggests heightened bed-stresses, also found by *Bogucki et al.* [1997].

4. Comparison to Theory

[12] We turn to soliton theory to make rough estimates for the phase speed and energy of the waves. We fit the waves using a fully non-linear method [*Turkington et al.*, 1991; *Lamb*, 2002] that uses as the background condition a flat bottom and laterally homogeneous stratification, and as input the observed amplitude of the waves (Figure 2). The method assumes that the waves have a permanent form moving with speed c. Solutions to Long's equation $(\nabla^2\eta + (N^2/c^2)\eta = 0)$ are found, where $\eta(x, z)$ is the distance the streamline at (x, z) has been displaced by the wave, and $N = N(z - \eta)$ is the stratification the streamline was originally at. Isopycnals slope up the shelf, so we used the stratification at −0.28 km for the first wave, and the stratification at −0.85 km for the last two. The predicted isopycnals are compared to the acoustic outline in Figure 5, dilated to account for the Doppler shift associated with the relative motion of the wave to the ship ($L' = LU_s/(U_s - c)$, where U_s is the ship speed ≈1.05 m s^{-1}).

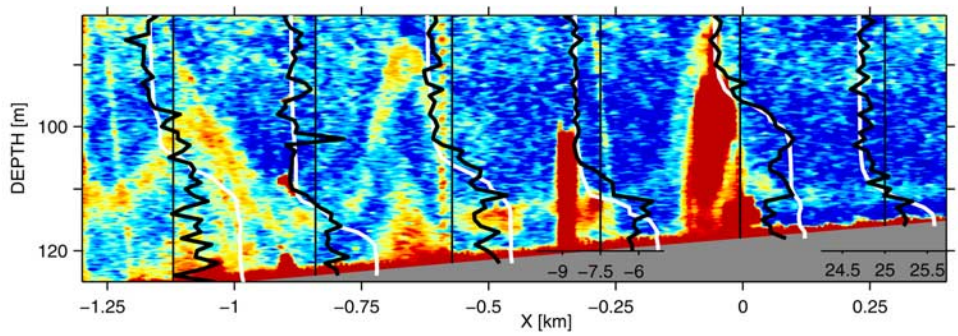

Figure 2. Internal solitary waves of elevation. 120 kHz echosounder image (red is high intensity and blue is low intensity). Data from chameleon drops are shown centered around the vertical lines. Density profiles (white) are centered at $\sigma_\theta = 25$ kg m^{-3} and dissipation profiles (black) are centered at $\log_{10}(\epsilon) = -7.5$.

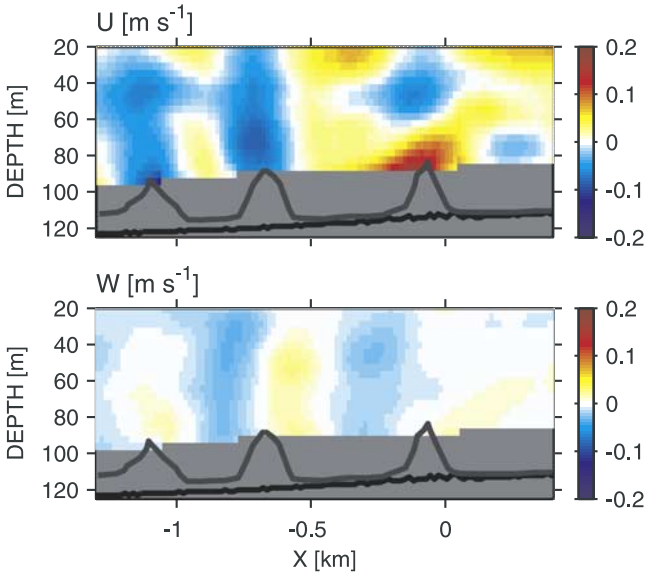

Figure 3. (a) Onshore and (b) vertical velocity above solitary waves. Grey trace is the approximate location of the scattering layer in Figure 2.

[13] The resulting solutions match the outline of the scattering layer relatively well, predicting that taller waves are also thinner. The phase speeds are on the order of 0.45 m s^{-1}, much faster than the linear phase speed of 0.2 m s^{-1}. However, acoustic scattering layers cross the simulated isopycnals, indicating that the fit waves are too wide. This is consistent with the behavior of shoaling waves, an effect not accounted for in the steady-state, flat bottom model used here, so the discrepancy is not surprising.

[14] Within the leading wave there is a region where the solution predicts closed streamlines, or a "trapped core," carried in the wave without contacting outside water [*Lamb*, 2002]. Observational evidence for a trapped core in the leading wave is fluid at 0 km that is denser than any observed at −0.25 km, a position through which the wave has already passed. The thick black contour in Figure 5 delineating the recirculating core encloses a region with a high density of biological scatterers. This is suggestive of onshore transport of both fluid and biology by the ISW.

5. Energetics

[15] The soliton solutions specify the velocity and density anomaly in the waves, thereby permitting estimates of their kinetic and available potential energies. The displacement η is calculated from the non-linear solver, and the stream-function is given by $\psi(x, z) = \psi_0(x, z - \eta)$, where $\psi_0(x, z) = cz$ is the stream function at infinity; density is calculated the same way. Velocity is calculated by $u = -\partial\psi/\partial z$ and $w = \partial\psi/\partial x$. $KE = 0.5\int\int \rho(u^2 + w^2)\, dx\, dz$. Background potential energy is calculated by resorting the density in each solution to a rest-state, giving a profile of background density $\rho_o(z)$ that is independent of x. $APE = \int\int g(\rho - \rho_o)z\, dx\, dz$. The kinetic energy is approximately double the potential energy for all three waves and the waves are rank ordered in terms of energy (Figure 5). The rate at which wave energy is dissipated via turbulence is estimated by integrating $\rho\epsilon$ ($\epsilon = 10^{-6}$ m^2 s^{-3}; note that 1 m^2 s^{-3} = 1 W kg^{-1}) over the area of the first wave, yielding a dissipation rate per unit along-shore distance of ≈1 W m^{-1}. This estimate represents a lower bound; the chameleon profiles did not resolve the waves, and none passed precisely through the middle of any of the waves where the near-bottom velocity (and presumably the turbulence) is highest. A possible upper bound is to assume that the dissipation scales as the cube of the near-bottom velocity, which yields an average dissipation rate in the wave approximately two times larger. The ratio of wave energy to this areally-integrated dissipation rate represents a time-scale related to the wave's decay due solely to turbulent dissipation. For the first wave, $E/\int \rho\epsilon\, dA$ results in dissipation time-scales between two and four days. Since the leading wave will reach the shore in 9 h at 0.45 m s^{-1}, the dissipative loss cannot control the distance these waves travel. Instead, we expect that these waves break farther up the sloping shelf.

[16] There are two likely sources of the turbulence in the waves. The solitary wave model indicates that the inverse Richardson number $Ri^{-1} = S^2/N^2$ is greater than the critical value of 4 through much of the interface, suggesting the potential for shear instability. This source of turbulence has been documented for near-surface ISWs of depression [i.e., *Moum et al.*, 2003]. A clear distinction between near-surface waves of depression and near-bottom waves of elevation is the requirement that the velocity in the bottom waves must vanish at the sea floor. This leads to a highly sheared bottom layer (not resolved in these measurements) and stress-driven turbulence.

[17] An estimate of bottom-stress can be made from our observed dissipation rate and bottom boundary layer similarity theory. *Dewey and Crawford* [1988] argue that the bottom stress is related to near-bottom dissipation by: $\tau_b = \rho(\kappa\epsilon z)^{2/3}$, where $\kappa = 0.4$. Our dissipation rates indicate that $5 \times 10^{-2} < \tau_b < 16 \times 10^{-2}$ Nm^{-2}. These are amongst the highest values of bed-stress estimated during summer cruises [*Perlin et al.*, 2003]. For comparison, the same wave on the surface would have a stress due to interaction with air of only $\tau_s \approx 5 \times 10^{-4}$ Nm^{-2} (derived from wind-stress estimates due to *Large and Pond* [1981]), two orders of magnitude smaller than for a bottom-trapped wave. This added stress at the sea floor is a significant difference between the ISWs observed here and those observed near the surface.

6. Summary and Discussion

[18] These observations show the presence of high amplitude ISWs of elevation propagating on-shore near

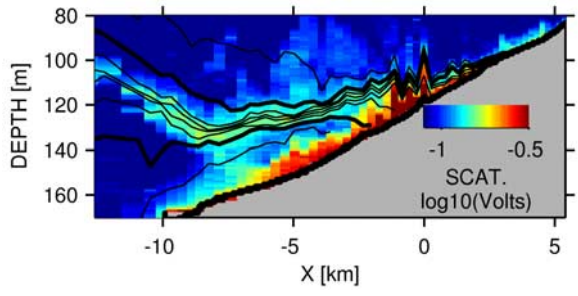

Figure 4. Section of 880 nm optical backscatter data from chameleon profiles.

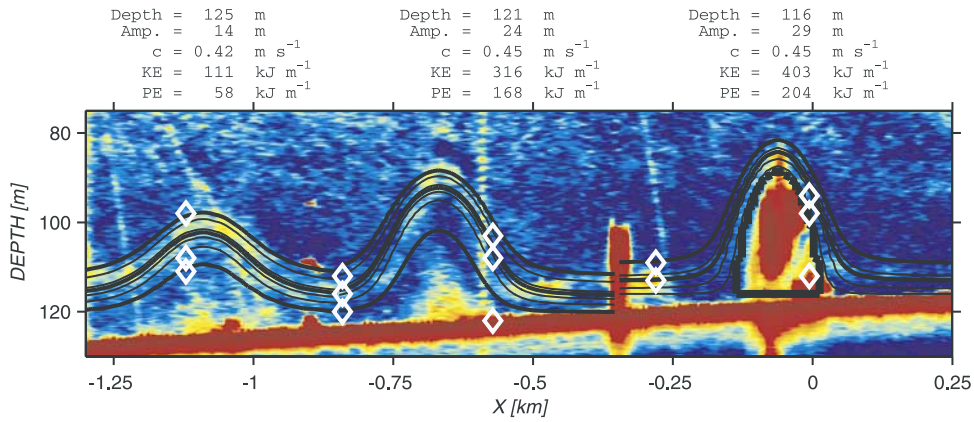

Figure 5. Isopycnals derived from the three soliton fits; thick isopycnals are $\sigma_\theta = 24.8, 25.25, 25.7$ kg m^{-3}. Parameters for the fits are shown above the image. White diamonds represent the depth of the thick isopycnals in the chameleon profiles. The closed thick black contour in the first wave indicates a recirculating core predicted by the non-linear fit.

the sea floor over the Oregon shelf. They are representative of a large number of similar wave trains observed during our 21-day cruise (to be presented in future papers). The common occurrence is likely due to the almost two-layer stratification with a thin lower layer that exists over the shelf at this time of the year [i.e., *Huyer et al.*, 1979].

[19] The waves are probably an important mechanism for transporting and mixing dense ocean water with the relatively homogeneous shelf water. The turbulence we observed is the highest outside of the surface mixed layer on the shelf, and is coincident with the highest stratification, implying large fluxes of buoyancy and other properties that have large cross-shelf gradients. We expect that the waves terminate in an abrupt manner further upshelf; if their termination is analogous to waves breaking on a beach, the resultant irreversible transport of fluid properties from the deep water will be large. The transport is enhanced if fluid is trapped in cores as suggested by the solitary wave solution.

[20] The high energy of the waves must be important for sediment resuspension [*Bogucki et al.*, 1997]. Our observations confirm the link between waves, turbulence, and high sediment load. The heightened resuspension probably acts to redistribute nutrients on the shelf, important to biological production, and the transport of pollutants. The heightened optical backscatter that extends in the front further off-shore suggests that this redistribution may be far-reaching.

[21] There are many unanswered questions about these waves. The non-linear solitary wave fit underestimates wave steepness, perhaps indicating the importance of wave shoaling. More fundamentally, we have many questions about the basic phenomena. How and where do the waves form? What is the role of tides in their generation? What is their eventual fate? How far up the shelf do they transport dense water (and accompanying sediment and nutrients), particularly if the water is in the trapped cores? These questions are the focus of further investigation.

[22] **Acknowledgments.** We thank Mike Neeley-Brown, Raymond Kreth, and Greig Thompson, and the captain and crew of the *R/V Revelle*. Kevin Lamb and Bill Smyth provided code and theoretical advice. Alexander Perlin performed the preliminary processing and with Jonathan Nash and Jennifer MacKinnon commented on early drafts. Two anonymous reviewers were very helpful in their comments, particularly by encouraging us to use a fully non-linear soliton solution rather than a weakly non-linear solution. Funding for the research was provided as part of the Coastal Ocean Advances in Shelf Transport project, NSF grant OCE-9907854.

References

Apel, J. R., J. R. Holbrook, A. K. Liu, and J. J. Tsia, The Sulu Sea internal soliton experiment, *J. Phys. Oceanogr.*, *15*, 1625–1651, 1985.

Bogucki, D., T. Dickey, and L. G. Redekopp, Sediment resuspension and mixing by resonantly generated internal solitary waves, *J. Phys. Oceanogr.*, *27*, 1181–1196, 1997.

Dewey, R. K., and W. R. Crawford, Bottom stress estimates from vertical dissipation rate profiles on the continental shelf, *J. Phys. Oceanogr.*, *18*, 1167–1177, 1988.

Huyer, A., E. J. C. Sobey, and R. L. Smith, The spring transition in currents over the Oregon continental shelf, *J. Geophys. Res.*, *84*, 6995–7011, 1979.

Lamb, K. G., Shoaling solitary internal waves: On a criterion for the formation of waves with trapped cores, *J. Fluid Mech.*, *478*, 81–100, 2002.

Large, W., and S. Pond, Open ocean momentum flux measurements in moderate to strong winds, *J. Phys. Oceanogr.*, *11*, 324–336, 1981.

Moum, J. N., M. C. Gregg, R. C. Lien, and M. Carr, Comparison of turbulence kinetic energy dissipation rate estimates from two ocean microstructure profilers, *J. Atmos. Ocean. Tech.*, *12*, 346–366, 1995.

Moum, J. N., D. M. Farmer, W. D. Smyth, L. Armi, and S. Vagle, Structure and generation of turbulence at interfaces strained by internal solitary waves propagating shoreward over the continental shelf, *J. Phys. Oceanogr.*, *33*, 2093–2112, 2003.

Perlin, A., J. N. Moum, and J. M. Klymak, Response of bottom boundary layer over the continental shelf to variations in alongshore wind, in preparation, 2003.

Seim, H. E., M. C. Gregg, and R. Miyamoto, Acoustic backscatter from turbulent microstructure, *J. Phys. Oceanogr.*, *12*, 367–380, 1995.

Turkington, B., A. Eydeland, and S. Wang, A computational method for solitary internal waves in a continuously stratified fluid, *Stud. Appl. Maths*, *85*, 93–127, 1991.

Wiebe, P. H., J. Irish, R. Beardsley, and T. Stanton, Observations of internal solitary waves on Georges Bank, in *EOS*, vol. 80, American Geophysical Union, 2000 Ocean Sciences Meeting, San Antonio, Texas, 24 –28 January, 2000.

J. M. Klymak and J. N. Moum, College of Ocean and Atoms. Sci., Oregon State University, 104 Ocean Admin Bldg., Corvallis, OR 97331-5503, USA. (jklymak@coas.oregonstate.edu)